Published in final edited form as:
*Neurobiol Dis*. 2009 May ; 34(2): 332–339. doi:10.1016/j.nbd.2009.02.003.

# A cellular model of Alzheimer's disease therapeutic efficacy: PKC activation reverses Aβ-induced biomarker abnormality on cultured fibroblasts

**Tapan K. Khan**[a,*], **Thomas J. Nelson**[a], **Vishal A. Verma**[c], **Paul A. Wender**[c,d], and **Daniel L. Alkon**[a,b]

a *Blanchette Rockefeller Neurosciences Institute, West Virginia University, School of Medicine, Morgantown, WV 26506, USA*

b *Department of Neurology, West Virginia University, School of Medicine, Robert C. Byrd Health Science Center, PO Box 9100, Morgantown, WV26506, USA*

c *Department of Chemistry, Stanford University, Stanford, CA 94305, USA*

d *Department of Chemical and Systems Biology, Stanford University, Stanford, CA 94305, USA*

## Abstract

PKC signaling is critical for the non-toxic degradation of amyloid precursor protein (APP) and inhibition of GSK3β, which controls phosphorylation of tau protein in Alzheimer's disease (AD). Thus the misregulation of PKC signaling could contribute to the origins of AD. Bryostatin, a potent PKC modulator, has the potential to ameliorate both the neurodegeneration and the recent memory loss associated with AD. As reported herein bryostatin and a potent synthetic analog (picolog) are found to cause stimulation of non-amyloidogenic pathways by increasing α-secretase activity and thus lowering the amount of toxic Aβ produced. Both bryostatin and picolog increased the secretion of the α-secretase product (s-APP-α) of APP at sub-nanomolar to nanomolar concentrations. A peripheral AD-Biomarker has previously been autopsy-validated. This Biomarker, based on bradykinin-induced differential phosphorylation of Erk1 and Erk2, has been used here to test the therapeutic efficacy both for bryostatin and picolog. Both of these PKC activators are then shown to convert the AD Erk1/2 phenotype of fibroblasts into the phenotype of "normal" control skin fibroblasts. This conversion occurred for both the abnormal Erk1/2 phenotype induced by application of $A\beta_{1–42}$ to the fibroblasts or the phenotype observed for fibroblasts of AD patients. The $A\beta_{1–42}$-induction, and PKC modulator reversal of the AD Erk1/2 biomarker phenotype demonstrate the AD-Biomarker's potential to monitor both disease progression and treatment response. Additionally, this first demonstration of the therapeutic potential in AD of a synthetically accessible bryostatin analog warrants further preclinical advancement.

### Keywords

Alzheimer's disease drug efficacy; Aβ; Bryostatin; α-Secretase; Biomarker; PKC; Skin fibroblasts; Erk; Synthetic analog of bryostatin

*Corresponding author. Fax: +1 301 294 7007. E-mail address: E-mail: tapan_khan@brni-jhu.org (T.K. Khan).

Disclosure

All authors disclose that there is no conflict and no financial interest. When applicable, appropriate approval and procedures were used concerning human subject.

## Introduction

Accumulating evidence indicates a series of AD pathophysiological abnormalities in tissues other than in the brain, including blood, skin fibroblasts, and ocular tissues. In AD skin fibroblasts, several cellular and molecular abnormalities were observed, such as fibroblast K + channels (Etcheberrigaray et al., 1993, 1994), PKC isozymes (Govoni et al, 1993; Favit et al., 1998), $Ca^{2+}$ signaling (Ito et al., 1994), MAP kinase Erk1/2 phosphorylation (Zhao et al., 2002; Khan and Alkon, 2006), and dysfunctional PP2A (Zhao et al., 2003). Gene expression studies using familial AD (FAD) skin fibroblasts showed that the disease process may even start before the onset of cognitive decline (Nagasaka et al., 2005). FAD fibroblasts were found to produce excess Aβ in culture fibroblasts (Citron et al., 1994; Johnston et al., 1994). More recently, a new autopsy-confirmed, internally controlled, phosphorylated Erk1/2 peripheral biomarker in skin fibroblasts has been introduced (Khan and Alkon, 2006; 2008).

Controlled activation of α-secretase to reduce Aβ formation offers an alternative strategy to reduce Aβ and possibly treat AD. Furthermore, PKCε activation also activates endothelin converting enzyme activity, which reduces amyloid plaque pathology in transgenic mice (Choi et al., 2006).

The macrocyclic lactone bryostatin, a natural product extracted from *Bugula neritina*, was found to activate PKC isozymes selectively (Etcheberrigaray et al., 2004). These PKC isozymes then activate *α*-secretases directly or through MAP kinase (Alkon et al., 2007). Due to the scarcity of bryostatin, its difficult isolation, and the complexity of the molecule, simplified and accessible synthetic analogs of bryostatin have been developed and have been found to be superior to bryostatin in some cases (Wender and Verma, 2008; Wender et al., 1998, 2002). In this study we showed that low concentrations (nM) of bryostatin and a synthetic analog termed, picolog, activated the non-amyloidogenic pathway by increasing the levels of α-secretase product(s). Both of these PKC activators were then shown to convert the AD Erk1/2 phenotype of fibroblasts into the phenotype of “normal” control skin fibroblasts. This conversion occurred for both the abnormal Erk1/2 phenotype induced by application of $A\beta_{1–42}$ to the fibroblasts or for the phenotype observed for fibroblasts of AD patients. These results indicate that the Erk1/2 biomarker may serve as model for monitoring drug efficacy and/or disease progression and that more accessible and tunable analogs of bryostatin can effectively emulate bryostatin’s role in the potential treatment of AD.

## Experiments

### Materials

Bradykinin (m.wt. 1060.2) was obtained from Calbiochem (San Diego, CA). Phospho-p44/p42 Erk1/2 antibodies from rabbit were purchased from Cell Signaling Technology (Danvers, MA). Secondary anti-rabbit antibody with peroxy conjugation was obtained from The Jackson Laboratories (Bar Harbor, ME). Bryostatin was purchased from Biomol International (Plymouth Meeting, PA). Amyloid beta ($A\beta_{1–42}$) was obtained from American Peptide Company (Sunnyvale, CA). 6E10 antibody (Covance, Emeryville, CA; formerly Signet Laboratories, Dedham, MA) was used to measure s-APP-α by Western blot.

### Cell culture

Banked skin fibroblasts from AD patients and age-matched control cases were purchased from Coriell Cell Repository (Camden, NJ). Cells were cultured and maintained in T25/T75 culture flasks with DMEM (high glucose) containing 10% fetal bovine serum and 100 U/mL penicillin and 100 μg/mL streptomycin. All cells were used within 7 to 16 passages.

### Preparation of bryostatin and picolog solutions

The designed, synthetic analog of bryostatin, picolog, was prepared according to published methods (Wender et al., 2002). Picolog's molecular structure is shown next to that of bryostain in Fig. 1. Picolog has been shown to bind with high affinity to PKC isozymes, translocate PKC-GFP fusion proteins in RBL cells, and suppress proliferation of various human cancer cells lines in a fashion comparable or superior to bryostatin. Picolog and bryostatin were dissolved in DMSO (50 μM) and aliquots were stored at −20 °C. Different concentrations of picolog and bryostatin solutions were prepared from these aliquots in regular medium just before each experiment.

### PKC activity assay

Each rat brain (Pel-Freez) was homogenized by sonication in 3 volumes of homogenization buffer (10 mM Tris-HCl pH 7.4, 50 mM NaF, 1 mM PMSF). Homogenates (100 μL) were incubated in triplicate for 5 min at 37 °C with PKC activator (bryostatin/picolog), then centrifuged at 100,000 ×g for 10 min. The precipitate was resuspended after sonication in the original volume. PKC activity was measured in 10 μL aliquots of supernatant and precipitated without added diacylglycerol or phosphatidylserine, measuring the incorporation of $^{32}P$ from ATP-γ-$^{32}P$ into histones as described previously (Nelson and Alkon, 1995). The ratio of PKC activity in the membrane to total PKC activity was used as an index of the degree of activation.

### Measurement of s-APP-α

Alzheimer's disease fibroblast cells (AG06848) were grown to 100% confluency in a 75 $cm^2$ culture flask. Culture medium was replaced by serum-free medium 2 h before the drug (bryostatin/picolog) treatment and kept in an incubator at 37 °C, 5% CO2. After 2 h, the serum free-medium was replaced by medium (3 mL) with appropriate concentration of drug (picolog/bryostatin) and kept in an incubator at 37 °C, 5% CO2. Treatment was maintained for 180 min. Upon completion of the treatment, the medium was collected and centrifuged at 1000 rpm for 5 min to remove any cellular debris. The supernatant was transferred into a pre-cooled labeled centrifuged tube, and immediately placed on ice and vortexed with 1/100 volume of 2% Na-deoxycholate (DOC) and placed at 4 °C for 30 min, precipitated by pre-cooled 100% trichloroacetic acid (1/10 volume of mixture) and kept overnight at 4 °C, spun at 20,000 ×g. The supernatant was removed and the pellet was washed in acetone and spun again at 20,000 ×g for 30 min at 4 °C. The supernatant was decanted and the pellet was dried overnight with parafilm with a very small hole on top to protect the samples from debris. The protein pellet was dissolved in 20 μl of homogenization buffer (100 mM Tris, pH7.4,150 mM NaCl, 1 mM EDTA, 1 mM EGTA, 0.5% NP-40, 1% Triton X-100, 1% protease inhibitor mixture, 1% phosphatase inhibitor cocktails). Twenty μl of 2× sample buffer was added and boiled in a water bath for 10 min. The resulting cocktails were loaded on 4–20% Tris–Glycine gels to conduct electrophoresis at 120 V for 80 min. Normalization of protein on each lane of the blots was done by loading equal volume of samples of conditioned medium standardized to total cell lysate protein concentration. This was followed by transfer of the protein onto a nitrocellulose membrane. After blocking the non-specific binding with 5% BSA for 1 h at room temperature, the antibody for s-APP-α (6E10, Covance, Emeryville, CA; formerly Signet Laboratories, Dedham, MA, 1:500 dilution), was added and incubated overnight on an end-to-end rocker at 4 °C. On the following day, the nitrocellulose membrane was washed three times (20 min each) with washing buffer (Bio-Rad Laboratories, Hercules, CA) with intermittent shaking at room temperature and incubated with an HRP-conjugated secondary antibody (Jackson Labs) for 1 h and followed by washing three times (20 min each) with washing buffer with intermittent shaking. The s-APP-α bands were stained with DAB (3,3 diaminobenzidine) staining.

### Therapeutic efficacy in a cellular model system

Therapeutic efficacy of bryostatin and picolog was tested with an autopsy-validated peripheral AD-Biomarker developed by our laboratory based on bradykinin-induced differential phosphorylation of Erk1 and Erk2 (Khan and Alkon, 2006, 2008) in human skin fibroblasts.

### Bryostatin and picolog treatment

Fibroblast cell lines from control patients were treated with 1.0 μM $A\beta_{1–42}$ (in DMEM culture medium with 10% fetal bovine serum), for 16 h in 5% CO2 and 37 °C after reaching 90–100% confluence. After the 16 h of incubation with $A\beta_{1–42}$, the medium was removed and washed three times with regular culture medium. Then an additional 16 h of incubation was conducted with 0.2 nM bryostatin/5 nM picolog in regular culture medium. The doses of both bryostatin and picolog were chosen based on the previously demonstrated potency of bryostatin at very low concentrations, i.e. within the sub-nanomolar range (Etcheberrigaray et al., PNAS 2004). The bryostatin concentration of 0.2 nM was previously chosen because of its maximum potency at that concentration. We then chose concentrations of picolog to compare potencies of picolog and bryostatin.

### Differential phosphorylation of Erk1/2

Confluent (90–100%) skin fibroblasts (Coriell Cell Repository, Camden, NJ) after bryostatin and picolog treatment were serum-deprived for 16 h. A 10 nM bradykinin (BK) challenge was conducted for 10 min (BK+). For each patient three pairs of BK and vehicle (DMSO, without BK, BK−) were measured. After the treatment, the medium was removed and the flasks were placed on dry ice/ethanol for 30 min. Homogenization buffer (100 mM Tris, pH 7.4, 150 mM NaCl, 1 mM EDTA, 1 mM EGTA, 0.5% NP-40,1% Triton X-100,1% protease inhibitor mixture, 1 % phosphatase inhibitor cocktail) was then added. The flasks were placed on an end-to-end rocker at 4 °C. After 30 min, cell extracts were collected with a cell scraper and sonicated three times on ice and kept on ice for 30 min. Cell lysates were centrifuged at 14,000 rpm (Eppendorf Centrifuge 5417R; Brinkman Instruments, Westbury, NY) for 15 min. The supernatants were used for Western blotting. The total number of cell passages was not allowed to exceed 16.

### Western blot analysis

Cell lysates were mixed with equal volumes of 2× SDS sample buffer and boiled for 10 min. The resulting cocktails were loaded on 10% gradient Tris-Glycine gels to conduct electrophoresis. This was followed by transfer of the protein onto a nitrocellulose membrane. After blocking the non-specific binding with nonfat milk for 1 h at room temperature, the blots were incubated with antibodies for total phospho-Erk1/2 measurements at 4 °C for 16 h. Blots were washed and the phospho-Erk signal was detected by ECL using anti-rabbit secondary antibodies from Jackson Laboratories and recorded on film. Blots were then stripped with stripping buffer and probed with the anti-Erk antibody and signals were recorded as above. Signal intensity was recorded with a BioRad densitometer. For Bradykinin-treated cells (BK +), both the P-Erk1 and P-Erk2 were elevated compared to untreated cells.

### AD-Index measurement

The AD-Index measurement was described elsewhere (Khan and Alkon, 2006, 2008). Strip densitometric analysis was conducted using Imul (http://brnineurosci.org/imul.html). Total intensities of P-Erk1 and P-Erk2 bands were measured separately. The ratios of P-Erk1 to P-Erk2 in the presence of BK (BK+) and in the absence of BK (BK−) were calculated separately. From these measurements, an Alzheimer's disease Index (AD-Index) was calculated as follows: AD-Index = $[\text{p-Erk1/p-Erk2}]^{BK+}-[\text{p-Erk1/p-Erk2}]^{BK-}$.

The AD-Index was measured for each control cell line before and after inducing the AD phenotype with 1.0 μM $A\beta_{1–42}$. After the $A\beta_{1–42}$ treatment the AD-Index was again measured before and after bryostatin/picolog treatment. For AD cell lines, the AD-Index was measured in a similar way, immediately before and after bryostatin (0.2 nM) or picolog (5 nM) treatment.

## Results

### Activation of α-secretase through PKC activation by bryostatin and picolog

It is well documented that at sub-nanomolar to nanomolar concentrations, bryostatin activates PKC. In comparison to bryostatin, picolog also activated PKC at nanomolar concentration (Fig. 2). However, at sub-nanomolar concentrations bryostatin was more potent than picolog. The α-secretase product (s-APP-α) was used as a measurement of α-secretase activity in AD skin fibroblasts. After bryostatin or picolog treatment the medium was collected and s-APP-α was assayed by a conventional immunobloting technique. In the range of sub-nanomolar to nanomolar concentrations, both bryostatin and picolog increased the secretion of the s-APP-α from amyloid precursor protein (APP) in AD skin fibroblasts (for bryostatin: 289±67 (SEM); for picolog: 160±29 (SEM) with respect to 100 for control, respectively). The production of s-APP-α by picolog was concentration-dependent (Figs. 3A(i) B). Bryostatin was found to be more potent for s-APP-α production at sub-nanomolar concentrations (Fig. 3C).

The 6E10 antibody that has been used in this study to detect s-APP-α secretion from human cell lines by Western blot analysis was described in numerous articles in the literature (Yang et al., 2007; Kozikowski et al., 2003; Sennvik et al., 2000; Petanceska and Gandy, 1999). These studies demonstrated that this antibody recognizes the 1–16 amino acid sequence of human Aβ. This region is absent in the β-secretase cleavage product (s-APP-β) of full length APP as was demonstrated in a study by Sennvik et al. (2000). The 6E10 antibody, also detects full length APP. However, the full length APP was not secreted by the cells into the medium, demonstrated by the lack of a band corresponding to the full length APP (Fig. 3A(i)). In our analyses we measured s-APP-α as secreted into the medium that was collected after centrifugation at 1000 rpm for 5 min to remove any cellular debris. In this way no APP (which remains with the cellular pellet) contaminated our measurements of s-APP-α. Therefore pertinent to this study, this antibody only detects s-APP-α that is specifically derived from α-secretase activity (Fig. 3A(ii)). The increase in s-APP-α depletes the amount of $A\beta_{1–40}$ as well as $A\beta_{1–42}$.

### Therapeutic efficacy in AD fibroblasts

Drug efficacy was tested using bradykinin induced differential phosphorylation of Erk1 and Erk2 and was followed by measuring the AD-Index. The AD-Index was measured for six different human AD skin fibroblasts as before (Khan and Alkon, 2006, 2008) and was found to be positive. Positive AD-Index values correspond to AD pathology. Both bryostatin (0.2 nM) and picolog (5 nM) treatment lowered the AD-Index values for AD fibroblasts, indicating that these compounds restored the healthy phenotype of AD fibroblasts (Figs. 4A and C). Corresponding AD-Index changes of individual cases have been illustrated in Figs. 4Band D .

### Therapeutic efficacy of bryostatin and picolog in control fibroblasts

Since the PKC activator, bryostatin, has shown both neuroprotective and cognitive enhancing efficacy, we tested the possibility that bryostatin might prevent the $A\beta_{1–42}$-induced abnormalities of the AD-Biomarker. Addition of 0.2 nM bryostatin protected against the $A\beta_{1–42}$-induced change of the AD-Biomarker into the positive values to normal AD-Index that would have indicated the presence of AD (Figs. 5A, B). After bryostatin treatment, the AD-Index values returned back to the normal lower values (*N*=6, AD-Index value changes from +0.130±0.035 to −0.034±0.049 (SEM)).

Similar results were obtained after picolog treatment (Figs. 5C and D). After soluble amyloidogenic $A\beta_{1-42}$ treatment (1 μM, 16 h), the fibroblasts were then found to have the AD-specific, positive AD-Biomarker values (*N*=4, AD-Index changes from −0.071 ± 0.035 (SEM) to +0.045±0.017 (SEM)). After picolog treatment, the positive AD-Index values produced by the treatment of $A\beta_{1-42}$ returned back to the normal lower values (AD-Index=−0.010±0.029 (SEM)) for control fibroblasts (Figs. 5C and D).

## Discussion

One of the most important histopathological hallmarks of AD is the presence of neuritic amyloid plaques or deposits of aggregated Aβ. Inhibiting excessive Aβ generation is also considered as one the most important therapeutic targets for AD drug development. Abnormal Aβ formation is a result of sequential proteolytic cleavage of transmembrane amyloid precursor protein (APP) by β- and γ-secretases. On the other hand, the non-amyloidogenic pathway activates α-secretase(s) that cause cleavage of APP within the Aβ sequence to generate s-APP-α, the soluble, non-toxic metabolic product. Modulation of these three secretase activities has received a great deal of attention for development of AD therapeutic strategies. Inhibition of β- and/or γ-secretases or activation of α-secretase pathways should decrease amyloid formation. However, γ-secretase has other essential substrates, such as Notch, Delta and Jagged (De Strooper et al., 1999) and inhibition of these could cause gastrointestinal problems and perhaps other side-effects (Milano et al., 2004). Inhibition of β-secretase would be more promising, and has been supported by several studies showing that knockout mice when crossed with amyloid generating mutant APP transgenic mice, are entirely resistant to amyloid accumulation (Luo et al., 2001). However, β-secretase other substrates as well, such as type III neuregulin 1 (NRG1), which is essential for nerve myelination and bundling axons (Willem et al., 2006; Glabe, 2006).

### Implications of synthetic analog of bryostatin

Bryostatin's ability to reverse the AD phenotype in fibroblasts, combined with its other known neurological effects such as the ability to increase memory and learning in various animal models, suggest that bryostatin could be an important therapeutic treatment for AD as well as other neurological conditions. However, the limited availability of active bryostatins from both natural sources (0.00014% isolation yield) as well as synthetic means (>70 steps) indicates that simplified, synthetically accessible and tunable bryostatin analogs would be invaluable in the search for equivalent or even superior agents. The ability of one such analog, picolog (<30 steps), to mimic bryostatin's efficacy in this study indicates that such analogs could be therapeutically significant and thus merit preclinical advancement.

### Secretase modulation therapeutic approach of AD

The therapeutic approaches for AD drug development to reduce Aβ can be categorized as: anti-amyloid treatments, anti-polymerization strategies, ion channel modulation approaches, and neuronal/cellular signaling modulation strategies. It is well documented that ion channel-modulating agents (e.g. acetylcholinesterase inhibitors (donepezil, rivastigmine etc), cholinergic receptor modulators (galantamine), and NMDA receptor antagonists (mematine)), cause modest symptomatic relief without providing disease modification. Anti-amyloid treatment can be performed with three different approaches: immunotherapeutic strategy, an anti-polymerizing strategy, and secretase modulation. Although immunotherapeutic approaches for transgenic mice model were effective, in human clinical trials, they failed due to T-cell mediated auto-immune responses (Orgogozo et al., 2003).

On the other hand, modulation of secretases offers an alternative strategy for decreasing Aβ formation by preventing transmembrane APP cleavage. APP is subject to post-translational

processing by three major enzyme systems (α-, β- and γ-secretases). Evidence has accumulated that inhibition of β- and/or γ-secretases decrease Aβ. However, γ- and β-secretases have other essential substrates such as Notch, inhibition of which can cause gastrointestinal problems (De Strooper et al., 1999; Milano et al., 2004) and NRG1 (essential for nerve myelination) (Willem et al., 2006; Glabe, 2006). In contrast, α-secretases cleave the APP to generate two non-toxic fragments, one of which is released extracellularly. The soluble form of APP-α (s-APP-α) is also neuroprotective and possibly synaptogenic. The α-secretases are potently regulated by PKC, particularly the α- and ε-isozymes (Lanni et al., 2004; Etcheberrigaray et al., 2004). PKC activation also has a crucial role in learning and memory enhancement (Sun and Alkon, 2005; Alkon et al., 2005). Conversely, inhibition of PKC consistently abolishes learning and memory retention. The strategy of PKC-mediated activation of α-secretases, therefore, has the advantage of three parallel beneficial consequences in AD therapy: increasing production of s-APP-α and reducing Aβ enhancing memory via PKC-mediated phosphorylation of downstream substrates, and decreasing phosphorylation of tau through inhibition of GSK-3β. Bryostatin-induced synaptogenesis for long-term associative memory is also regulated by PKC activation (Hongpaisan and Alkon, 2007).

## Soluble Aβ induces and picolog treatment reverses the Alzheimer's phenotype of human fibroblasts

Accumulating evidence suggests that soluble $A\beta_{1–42}$ can induce some of the neuropathology both with *in vitro* (brain slice) and *in vivo* administration (Sun and Alkon, 2002). Furthermore, *in vivo* infusion of $A\beta_{25–35}$ (an active form of $A\beta_{1–42}$) can also induce learning and memory impairments that are characteristic of early AD patients (Sun and Alkon, 2002). In addition, for familial AD patients, skin fibroblasts showed enhanced secretion of $A\beta_{1–42}$ (Citron et al., 1994; Johnston et al., 1994) while AD-specific reduction of specific K+ channels were induced by $A\beta_{1–42}$ in normal human fibroblasts (Etcheberrigaray et al., 1993, 1994). For these reasons, we applied $A\beta_{1–42}$ to the normal fibroblasts to assess its impact on Erk1/2 phosphorylation. The AD-Index was first measured for these control fibroblasts and was found to have the expected negative (normal) values of the AD-Index. After soluble $A\beta_{1–42}$ treatment (1 μM, overnight), the fibroblasts were then found to have the AD-specific positive AD-Biomarker.

Since the PKC activator bryostatin had shown both neuroprotective (in double transgenic mice) and cognitive enhancing efficacy, we then tested the possibility that bryostatin might prevent the $A\beta_{1–42}$-induced abnormalities of the AD-Biomarker. As predicted, addition of 0.2 nM bryostatin (Khan and Alkon, 2008) or 5 nM picolog (Fig. 5) prevented the $A\beta_{1–42}$-induced change of the AD-Biomarker into the positive values that would have indicated the presence of AD. Similar to bryostatin from our previous study (Khan and Alkon, 2008), picolog also reversed the abnormal Erk1/2 phenotype of AD fibroblasts. Such results demonstrate that the PKC activators, bryostatin and picolog, have the potential to ameliorate both the neurodegeneration and the recent memory loss of AD, and offer evidence for the hypothesis that PKC signaling deficits may themselves contribute to the origins of AD.

## Possible underlying mechanism of α-sectretase activation and its relationship to the AD-Index measurement

First, we hypothesize that the AD-Biomarker shows enhanced Erk1/2 phosphorylation in response to bradykinin because AD patients already have reduced levels of PKCα/ε-mediated phosphorylation of Erk1/2 as illustrated in our previous work (Khan and Alkon, 2006). When challenged with PKC activation, the AD fibroblasts show an increased dynamic change of Erk1/2 phosphorylation because they are starting from a decreased steady state level. Aβ application to normal fibroblasts reduces PKC activity because Aβ directly down-regulates PKC, as has been previously demonstrated (Favit et al., 1998; Lee et al., 2004). In this way, Aβ application would simulate AD (Fig. 6). PKC activators such as bryostatin and picolog

would counteract the effect of Aβ and thereby reverse or prevent the Aβ-induced changes of AD-Index (Fig. 6). Other effects of AD-specific lowering of PKC isozymes might induce reduced α-secretase activity and/or reduced endothelin-converting enzyme degradation of Aβ. However, the relationship of the AD-Index to other effects of PKC reduction is not explored in the present study.

It would be interesting to examine the AD-Index in AD fibroblasts after inhibiting γ-secretase and this will be examined in future studies. If γ-secretase activity is inhibited, we expect lower amounts of Aβ production and as a result lower AD-Index value as compare to values obtained without γ-secretase inhibition.

### Drug efficacy in a cellular model

Values of the AD-Biomarker (AD-Index) were measured for control fibroblasts and were found to have the negative (normal) values of the AD-Biomarker. After soluble amyloidogenic $A\beta_{1–42}$ treatment (1 μM, 16 h), the fibroblasts were then found to have the AD-specific, positive AD-Index values. Since the PKC activator, bryostatin, has shown both neuroprotective and cognitive enhancing efficacy, we then tested the possibility that picolog might prevent the $A\beta_{1–42}$ induced abnormalities of the AD-Biomarker. Addition of 5 nM picolog protected against the $A\beta_{1–42}$-induced change of the AD-Biomarker into the positive values that would have indicated the presence of AD (see above). Both bryostatin (0.2 nM) and picolog (5 nM) treatment lowered the AD-Index values for AD fibroblasts, indicating that these compounds restore the healthy phenotype of AD fibroblasts as well as have the potential for use as AD treatments.

A growing body of evidence indicates that AD pathophysiological abnormalities occur in the brain as well as in blood and blood vessels, skin fibroblasts and ocular tissues. PKC signaling was found to be critical for non-toxic degradation of APP directly and/or through MAPK (Alkon et al., 2007). The AD-phenotype and/or AD-Index of skin fibroblasts are correlated with AD neuropathology of brain. Recent findings from our laboratory showed that the AD-Index values of autopsy-confirmed patients were correlated with AD neuropathology of amyloid plaques and fibrilliary tangles (Khan and Alkon, 2006, 2008). The amelioration of the AD-Index by bryostatin/picolog by itself does not directly indicate that the neuropathology will be ameliorated. However, bryostatin treatment of AD transgenic mice lowered Aβ in the brain and increasing survival rate (Etcheberrigaray et al., 2004). Similarly, treatment of AD transgenic mice by picolog and other accessible and tunable analogs would be critical to examine for effects on Aβ and amyloid plaques for further clinical development of these novel agents.

Thus, the AD-Biomarker successfully follows the bryostatin and picolog induced PKC-mediated transformation of cellular signaling in AD fibroblasts. These results suggest that the AD-Index measured in human fibroblasts could reflect therapeutic efficacy in cellular systems. PKC signaling deficits may contribute to the origins of Alzheimer's disease, so screening of PKC activators with the AD-Index measurement may provide a basis for rapid drug screening, at least at the early stages of AD drug development. This method would avoid lumbar puncture required by CSF biomarker for drug screening and efficacy testing.

## Acknowledgements

This study was supported by the intramural grants of Blanchette Rockefeller Neurosciences Institute (BRNI) to TKK and DLA, and NIH National Cancer Institute (CA31845) to PAW.

## References


Alkon DL, Epstein H, Kuzirian A, Bennett MC, Nelson TJ. Protein synthesis required for long-term memory is induced by PKC activation on days before associative learning. Proc Natl Acad Sci USA 2005;102:16432–16437. [PubMed: 16258064]

Alkon DL, Sun MK, Nelson TJ. PKC signaling deficits: a mechanistic hypothesis for the origins of Alzheimer's disease. Trends Pharmacol Sci 2007;28:51–60. [PubMed: 17218018]

Choi DS, Wang D, Yu GQ, Zhu G, Kharazia VN, Paredes JP, Chang WS, Deitchman JK, Mucke L, Messing RO. PKCε increases endothelin converting enzyme activity and reduces amyloid plaque pathology in transgenic mice. Proc Natl Acad Sci USA 2006;103:8215–8220. [PubMed: 16698938]

Citron M, Vigo-Pelfrey C, Teplow DB, Miller C, Schenk D, Johnston J, Winblad B, Venizelos N, Lannfelt L, Selkoe DJ. Excessive production of amyloid beta-protein by peripheral cells of symptomatic and presymptomatic patients carrying the Swedish familial Alzheimer disease mutation. Proc Natl Acad Sci USA 1994;91:11993–11997. [PubMed: 7991571]

De Strooper B, Annaert W, Cupers P, Saftig P, Craessaerts K, Mumm JS, Schroeter EH, Schrijvers V, Wolfe MS, Ray WJ, Goate A, Kopan R. A presenilin-1-dependent gamma-secretase-like protease mediates release of Notch intracellular domain. Nature 1999;398:518–522. [PubMed: 10206645]

Etcheberrigaray R, Ito E, Oka K, Tofel-Grehl B, Gibson GE, Alkon DL. Potassium channel dysfunction in fibroblasts identifies patients with Alzheimer disease. Proc Natl Acad Sci USA 1993;90:8209–8213. [PubMed: 8367484]

Etcheberrigaray R, Ito E, Kim CS, Alkon DL. Soluble beta-amyloid induction of Alzheimer's phenotype for human fibroblast K+ channels. Science 1994;264:276–279. [PubMed: 8146663]

Etcheberrigaray R, Tan M, Dewachter I, Kuipéri C, Van der AI, Wera S, Qiao L, Bank B, Nelson TJ, Kozikowski AP, Van Leuven F, Alkon DL. Therapeutic effects of PKC activators in Alzheimer's disease transgenic mice. Proc Natl Acad Sci USA 2004;101:11141–11146. [PubMed: 15263077]

Favit A, Grimaldi M, Nelson TJ, Alkon DL. Alzheimer's-specific effects of soluble beta-amyloid on protein kinase C-alpha and -gamma degradation in human fibroblasts. Proc Natl Acad Sci USA 1998;95:5562–5567. [PubMed: 9576922]

Glabe C. Avoiding collateral damage in Alzheimer's disease treatment. Science 2006;314:602–603. [PubMed: 17068248]

Govoni S, Bergamaschi S, Racchi M, Battaini F, Binetti G, Bianchetti A, Trabucchi M. Cytosol protein kinase C downregulation in fibroblasts from Alzheimer's disease patients. Neurology 1993;43:2581–2586. [PubMed: 8255461]

Hongpaisan J, Alkon DL. A structural basis for enhancement of long-term associative memory in single dendritic spines regulated by PKC. Proc Natl Acad Sci USA 2007;104:19571–19576. [PubMed: 18073185]

Ito E, Oka K, Etcheberrigaray R, Nelson TJ, McPhie DL, Tofel-Grehl B, Gibson GE, Alkon DL. Internal Ca2+ mobilization is altered in fibroblasts from patients with Alzheimer disease. Proc Natl Acad Sci USA 1994;91:534–538. [PubMed: 8290560]

Johnston JA, Cowburn RF, Norgren S, Wiehager B, Venizelos N, Winblad B, Vigo-Pelfrey C, Schenk D, Lannfelt L, O'Neill C. Increased beta-amyloid release and levels of amyloid precursor protein (APP) in fibroblast cell lines from family members with the Swedish Alzheimer's disease APP670/671 mutation. FEES Lett 1994;354:274–2748.

Khan TK, Alkon DL. An internally controlled peripheral biomarker for Alzheimer's disease: Erk1 and Erk2 responses to the inflammatory signal bradykinin. Proc Natl Acad Sci USA 2006;103:13203–13207. [PubMed: 16920798]

Khan TK, Alkon DL. Early diagnostic accuracy and pathophysiologic relevance of an autopsy-confirmed Alzheimer's disease peripheral biomarker. Neurobiol Aging. 200810.1016/j.neurobiolaging.2008.07.010

Kozikowski AP, Nowak I, Petukhov PA, Etcheberrigaray R, Mohamed A, Tan M, Lewin N, Hennings H, Pearce LL, Blumberg PM. New amide-bearing benzolactam-based protein kinase C modulators induce enhanced secretion of the amyloid precursor protein metabolite sAPPα. J Med Chem 2003;46:364–373. [PubMed: 12540236]

Lanni C, Mazzucchelli M, Porrello E, Govoni S, Racchi M. Differential involvement of protein kinase C alpha and epsilon in the regulated secretion of soluble amyloid precursor protein. Eur J Biochem 2004;271:3068–3075. [PubMed: 15233804]

Lee W, Boo JH, Jung MW, Park SD, Kim YH, Kim SU, Mook-Jung I. Amyloid beta peptide directly inhibits PKC activation. Mol Cell Neurosci 2004;26:222–231. [PubMed: 15207847]

Luo Y, Bolon B, Kahn S, Bennett BD, Babu-Khan S, Denis P, Fan W, Kha H, Zhang J, Gong Y, Martin L, Louis JC, Van Q, Richards WG, Citron M, Vassar R. Mice deficient in BACE1, the Alzheimer's beta-secretase, have normal phenotype and abolished beta-amyloid generation. Nat Neurosci 2001;4:231–232. [PubMed: 11224535]

Milano J, McKay J, Dagenais C, Foster-Brown L, Pognan F, Gadient R, Jacobs RT, Zacco A, Greenberg B, Ciaccio PJ. Modulation of notch processing by gamma-secretase inhibitors causes intestinal goblet cell metaplasia and induction of genes known to specify gut secretory lineage differentiation. Toxicol Sci 2004;82:341–358. [PubMed: 15319485]

Nagasaka Y, Dillner K, Ebise H, Teramoto R, Nakagawa H, Lilius L, Axelman K, Forsell C, Ito A, Winblad B, Kimura T, Graff C. A unique gene expression signature discriminates familial Alzheimer's disease mutation carriers from their wild-type siblings. Proc Natl Acad Sci USA 2005;102:14854–148549. [PubMed: 16199521]

Nelson TJ, Alkon DL. Phosphorylation of the conditioning-associated GTP-binding protein cp20 by protein kinase. C J Neurochem 1995;65:2350–2357.

Orgogozo JM, Gilman S, Dartigues JF, Laurent B, Fuel M, Kirby LC, Jouanny P, Dubois B, Eisner L, Fitman S, Michel BF, Boada M, Frank A, Hock C. Subacute meningoencephalitis in a subset of patients with AD after Abeta42 immunization. Neurology 2003;61:46–54. [PubMed: 12847155]

Petanceska SS, Gandy S. The phosphatidylinositol 3-kinase inhibitor wortmannin alters the metabolism of the Alzheimer's amyloid precursor protein. J Neurochem 1999;73:2316–2320. [PubMed: 10582589]

Sennvik K, Fastbom J, Blomberg M, Wahlund LO, Winblad B, Benedikz E. Levels of alpha- and beta-secretase cleaved amyloid precursor protein in the cerebrospinal fluid of Alzheimer's disease patients. Neurosci Lett 2000;278:169–172. [PubMed: 10653020]

Sun MK, Alkon DL. Impairment of hippocampal CA1 heterosynaptic transformation and spatial memory by beta-amyloid (25–35). J Neurophysiol 2002;87:2441–2449. [PubMed: 11976381]

Sun MK, Alkon DL. Dual effects of bryostatin-1 on spatial memory and depression. Eur J Pharmacol 2005;512:43–51. [PubMed: 15814089]

Wender PA, Verma VA. The design, synthesis, and evaluation of C7 diversified bryostatin analogs revels a hotspot for PKC affinity. Org Lett 2008;10:3331–3334. [PubMed: 18588309]

Wender PA, Baryza JL, Bennett CE, Bi FC, Brenner SE, Clarke MO, Horan JC, Kan C, Lacôte E, Lippa B, Nell PG, Turner TM. The practical synthesis of a novel and highly potent analogue of bryostatin. J Am Chem Soc 2002;124:13648–13649. [PubMed: 12431074]

Wender PA, DeBrabander J, Harran PG, Jimenez JM, Koehler MF, Lippa B, Park CM, Siedenbiedel C, Pettit GR. The design, computer modeling, solution structure, and biological evaluation of synthetic analogs of bryostatin 1. Proc Natl Acad Sci USA 1998;95:6624–6629. [PubMed: 9618462]

Willem M, Garratt AN, Novak B, Citron M, Kaufmann S, Rittger A, DeStrooper B, Saftig P, Birchmeier C, Haass C. Control of peripheral nerve myelination by the beta-secretase BACE1. Science 2006;314:664–666. [PubMed: 16990514]

Yang HQ, Pan J, Ba MW, Sun ZK, Ma GZ, Lu GQ, Xiao Q, Chen SD. New protein kinase C activator regulates amyloid precursor protein processing in vitro by increasing α-secretase activity. Eur J Neurosci 2007;26:381–391. [PubMed: 17650113]

Zhao WQ, Ravindranath L, Mohamed AS, Zohar O, Chen GH, Lyketsos CG, Etcheberrigaray R, Alkon DL. MAP kinase signaling cascade dysfunction specific to Alzheimer's disease in fibroblasts. Neurobiol Dis 2002;11:166–183. [PubMed: 12460556]

Zhao WQ, Feng C, Alkon DL. Impairment of phosphatase 2A contributes to the prolonged MAP kinase phosphorylation in Alzheimer's disease fibroblasts. Neurobiol Dis 2003;14:458–469. [PubMed: 14678762]

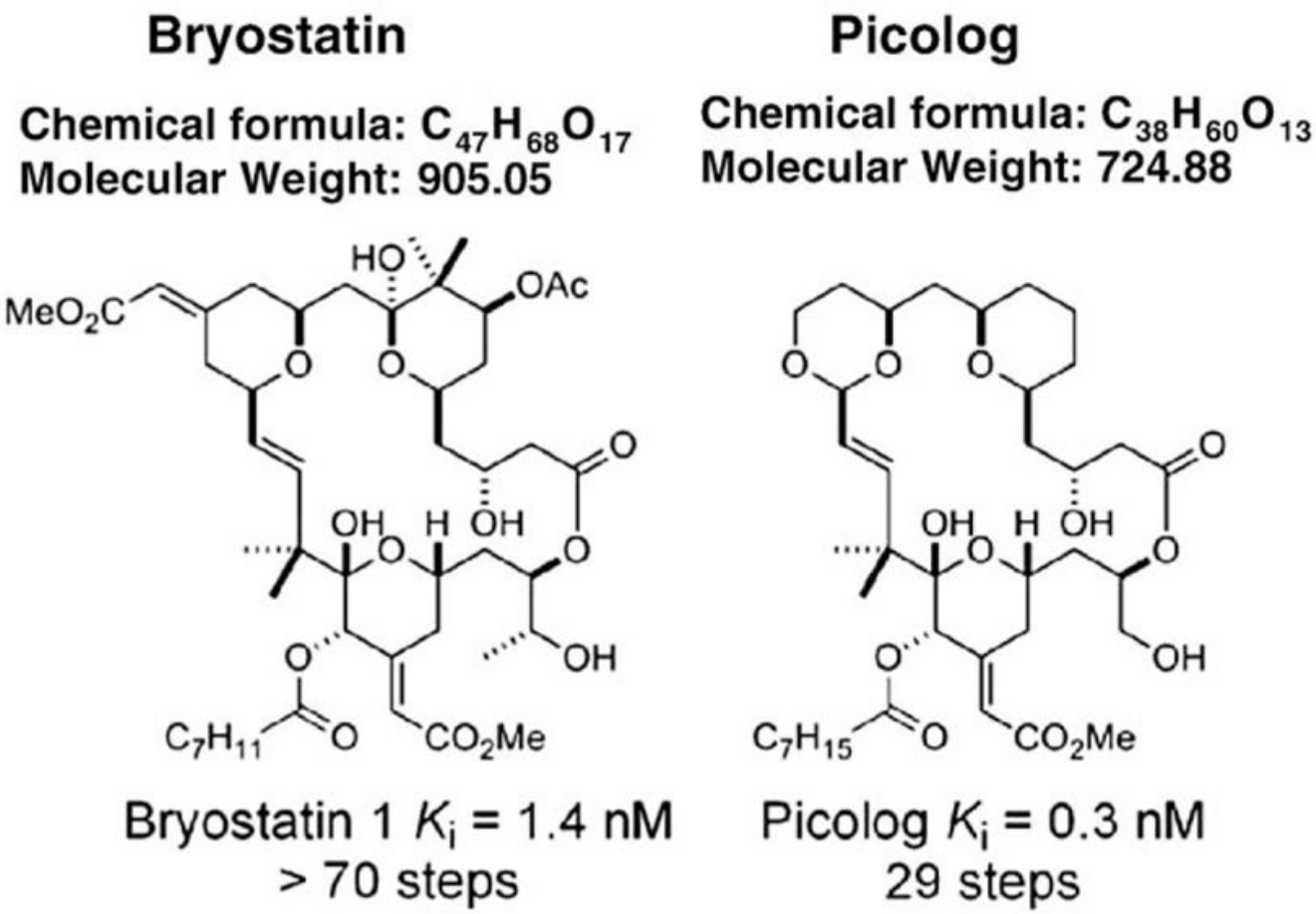


**Fig. 1.**
Chemical formula of bryostatin and picolog.

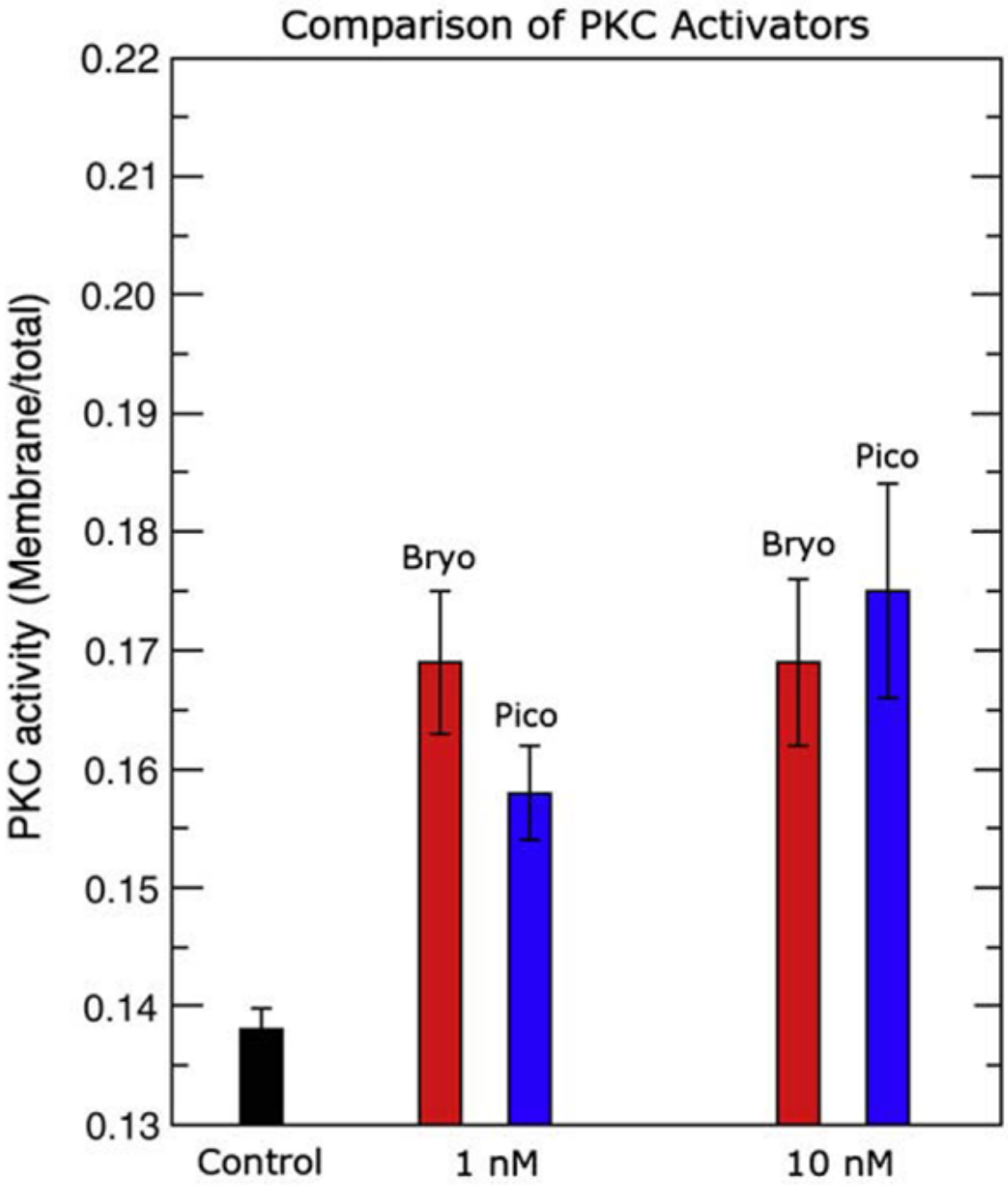


**Fig. 2.**
PKC activation by bryostatin and synthetic analog, picolog.

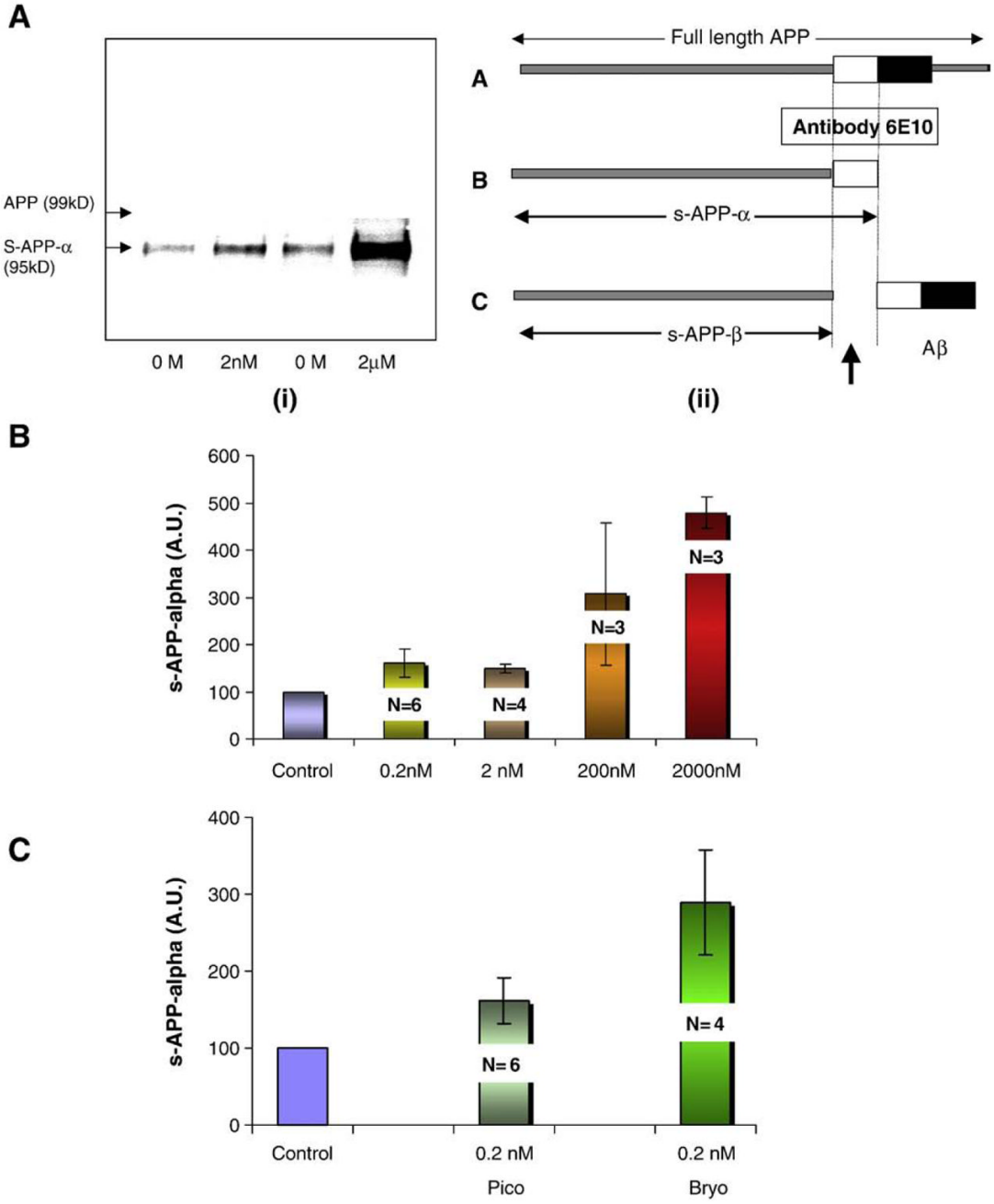


**Fig. 3.**

Increase of α-secretase activity by picolog Alzheimer's disease fibroblasts: (A) (i) Western blot analysis of secretion of s-APP-α by picolog treatment, (ii) Illustration of recognition of s-APP-α by 6E10 antibody. (B) Concentration dependence of α-secretase product formation (s-APP-α) by picolog. (C) Comparison of α-secretase activity induced by sub-nanomolar concentrations of bryostatin and picolog. (*N*=Number of independent measurements, **P*<0.028).

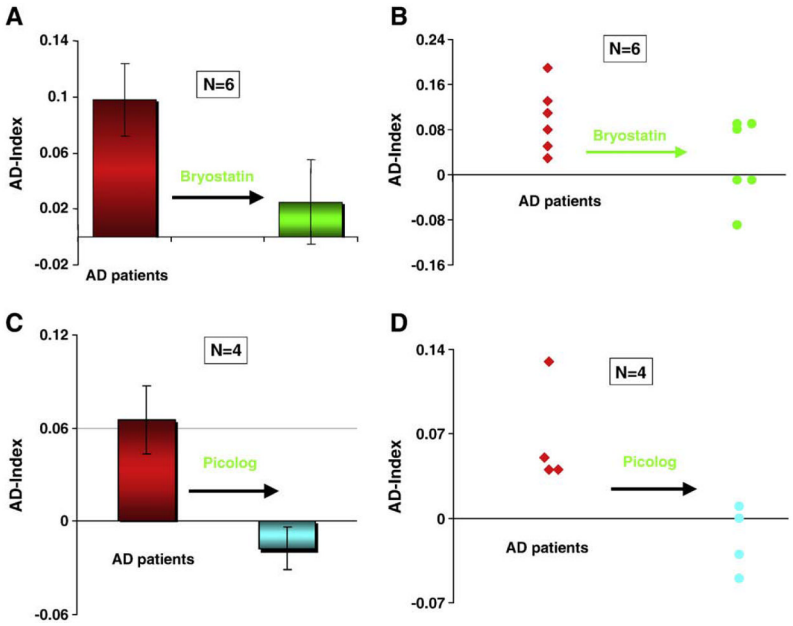


**Fig. 4.**

Bryostatin and picolog treatment reverses AD-Index of human Alzheimer's disease fibroblasts: (A) Skin fibroblasts cells from AD patients were treated with 0.2 nM bryostatin for 16 h. AD-Index was measured before and after the treatment and found to be decreased after each treatment. (*N*=Number of skin fibroblast from individual patient cell lines, **P*<0.02, Error bars=SEM of all AD-Index values). (B) Scatterplot of individual data points from each cell lines of panel A. (C) Skin fibroblasts cells from AD patients were treated with 5 nM picolog for 16 h in culture medium. AD-Index was measured before and after the treatment and found to be decreased after each treatment. (*N*=Number of skin fibroblast from individual patient cell lines, **P*<0.008, Error bars=SEM of all AD-Index values). (D) Scatterplot of individual data points from each cell lines of panel C

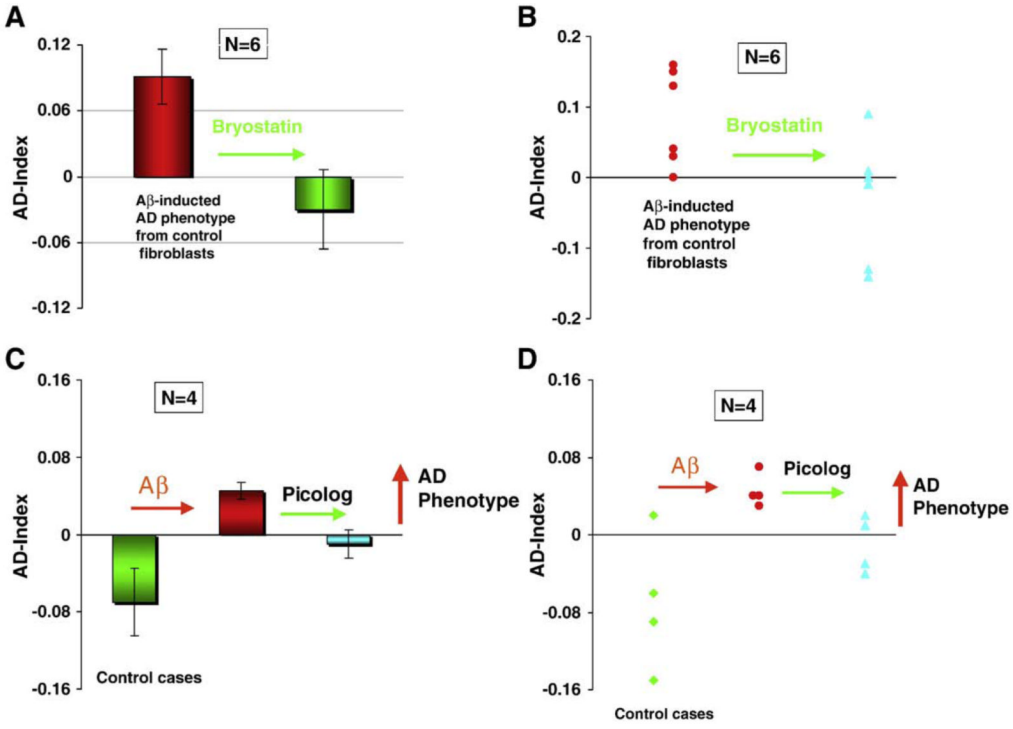


**Fig. 5.**

Bryostatin/picolog treatment reverses AD-Index of $A\beta_{1-42}$-treated control fibroblasts: (A) Skin fibroblasts from control patients were treated with 1.0 μM $A\beta_{1-42}$ in culture medium for 16 h to produce the AD phenotype. After $A\beta_{1-42}$-treatment, the AD phenotype skin fibroblasts were exposed with 0.2 nM bryostatin in culture medium for 16 h. The abnormal AD-Index was reversed to normal (negative) values. (*N*=Number of skin fibroblast from individual patient cell lines, $P < 0.005$). (B) Scatterplot of individual data points from each cell lines of panel A. (C) The skin fibroblasts from control patients were treated with 1.0 μM $A\beta_{1-42}$ for 16 h in culture medium to produce the AD phenotype. After $A\beta_{1-42}$-treatment, the AD phenotype skin fibroblasts were exposed to 5 nM picolog in culture medium for 16 h. The abnormal AD-Index was reversed to normal (negative) values. *(N*=Number of skin fibroblast from individual patient cell lines, $*P<0.01$, $**P<0.01$). (D) Scatterplot of individual data points from each cell lines of panel C.

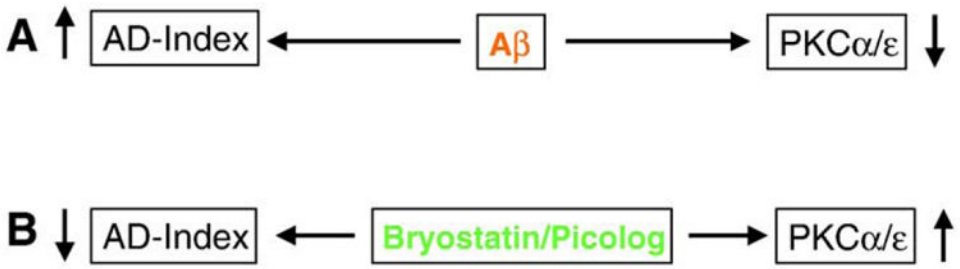


**Fig. 6.**
Illustration of effects of Aβ and PKC activators (bryostatin and picolog) on the AD-Index.